La mer 38 : 211–218, 2000
Société franco-japonaise d'océanographie, Tokyo

Water, heat and salt transports from diagnostic world ocean and north pacific circulation models

Zexun WEI* Byung-Ho CHOI** and Guohong FANG*

Abstract : Global and North Pacific robust diagnostic models are established based on MOM of GFDL to study the circulation in the world ocean and East Asian marginal seas respectively. The horizontal grid sizes are 1 degree for the global model and 1/3 degree for the North Pacific model, and the vertical water column is divided into 21 levels. The hydrographic data are taken from World Ocean Atlas 1994 (1994) and the wind stress from HELLERMAN and ROSENSTEIN (1983).

Based on the model result, the horizontal volume, heat and salt transports across some representative sections are calculated. The results show that: though the cross-equator volume transports in the Atlantic, Indian and Pacific Oceans are all small, the heat transports across equator in the Atrantic is northward. This is cleary a result of the southward flow of the North Atrantic Deep Water and the northward compensating warm flow in the upper layer. The annual mean of the cross-equator heat transport in the Pacific from the present model is significantly lower than that calculated by PHILANDER *et al.* (1987). This might indicate the importance of the Indonesian Throughflow in the heat transport in the Pacific. Our calculation shows that the heat transport through the Indonesian Archipelago is −1.0 PW, which is comparable with the poleward heat transport in the North Atlantic and Pacific Oceans. The difference in heat transports across the sections 4 (it separates the southern Atlantic and Indian oceans) and 5 (it separates the southern Pacific and Atlantic Oceans) demonstrates the importatn role of tha Agulhas current in the heat balance of the world ocean.

Key words : *Volume transport, heat transport, salt transport, world ocean*

1. Introduction

The rapid development of the computers has made it possible to simulate the ocean circulation using three dimension primitive numerical models, especially for the large margin with fine resolution. GFDL (Feophysical Fluid Dynamic Laboratory)'s Modular Ocean Model (MOM) is one of this kind of models. It is based on Kirk BRYAN (1969)'s work. As described by Bryan, the equations consist of the Navier Stokes equations subject to the Boussinesq, hydrostatic, and rigid lid approximations along with a nonlinear equation of state which couples two active tracers, temperature and salinity to the fluid velocity.

* Department of Physical Oceanography, Institute of Oceanology, Chinese Academy of Sciences, 7 Nanhai Road, Qingdao 266071, China (e-mail: weizx@ms.qdio.ac.cn)

** Department of Civil and Environmental Engineering, Sungkyunkwan University, Korea

The diagnostic study on the world ocean circulation has been conducted by FUJIO *et al.* (1991, 1992). The resolution of their model was $2° \times 2°$, thus it was not able to resolbe the East Asian marginal seas adequately and the emphasis of their study was on the water movement.

In the present study, we established a $1° \times 1°$ resolution robust diagnostic model for the world ocean and $1°/3 \times 1°/3$ resolution robust diagnostic model for the North Pacific ocean based on MOM to study the circulation on the world ocean and East Asian marginal seas respectively. Based on the model results, the horizontal volume, heat and salt transports across some representative sections are obtained.

2. Model description

The governing equations are as follows:

$$\frac{\partial u}{\partial t}+(u\cdot\nabla)u+w\frac{\partial u}{\partial z}+fk\times u$$
$$=-\frac{1}{\varrho_0}\nabla p+A_H\nabla^2 u \quad (1)$$
$$+A_v\frac{\partial^2 u}{\partial z^2}+minor\quad terms$$

$$\frac{\partial p}{\partial z}+\rho g=0 \quad (2)$$

$$\nabla\cdot u+\frac{\partial w}{\partial z}=0 \quad (3)$$

$$\frac{\partial\theta}{\partial t}+(u\cdot\nabla)\theta+w\frac{\partial\theta}{\partial z}$$
$$=K_H\nabla^2\theta+K_v\frac{\partial^2\theta}{\partial z^2}+\gamma(\theta^*-\theta) \quad (4)$$

$$\frac{\partial S}{\partial t}+(u\cdot\nabla)S+w\frac{\partial S}{\partial z}$$
$$=K_H\nabla^2 S+K_v\frac{\partial^2 S}{\partial z^2}+\gamma(S^*-S) \quad (5)$$

$$f=2\Omega\sin\phi \quad (6)$$

The damping terms $\gamma(\theta^*-\theta)$ and $\gamma(S^*-S)$ in the equations (4) and (5) were first proposed by SARMIENTO and BRYAN (1982), and the model was called as *robust diagnostic* model. These terms force the model-produced temperature ad salinity to approach the observed values.

The horizontal resolution is 1 degree for the global model and 1/3 degree for the North Pacific model, and the vertical water column is divided into 21 levels (see Table 1). The domain is 0°-360°, 80°S-87°N for the Global model and 99°E-75°W, 2°N-64°N for the North Pacific model. The topography is taken from DBDB5 data set (Natinal Geophysical Data Center, Boulder, Colorado). The hydrographic data is taken from World Ocean Atlas 1994 (1994) and the wind stress from HELLERMAN and ROSENSTEIN (1983).

The damping coefficient γ was taken:

$$\gamma=[\gamma_d+(\gamma_0-\gamma_d)*e^{\frac{z}{h}}]*|\sin\varphi| \quad (7)$$

where γ_0 and γ_d are the coefficients at the sea surface and abyss, set as $(100\text{day})^{-1}$ and $1/5\gamma_0$ respectively. z is the water depth, $h=500$ m, φ is the latitude. To restore the observed temperature and salinity quickly, we used larger γ during the first month integration.

As shown in FUJIO *et al.* (1992), the diagnostic model is not significantly influenced by the choice of eddy mixing parameters. Thus we used the following values:

$$A_H=1.0\times10^8\ \text{cm}^2/\text{s},\ A_V=1.0\ \text{cm}^2/\text{s},$$
$$K_H=1.0\times10^7\ \text{cm}^2/\text{s},\ K_V=0.2\ \text{cm}^2/\text{s}.$$

In the global model, we used the cyclic boundary condition on the east and west boundaries, and the solid boundary conditons on the north and south boundaries. In the North Pacific model, we used the solid boundary conditions on the all boundaries. The Bering Strait lies on the north, but the volume transport is very small. The south boundary is open, but the current here is basically zonal, therefore, to simplify the problem, we neglect the meridional flows along these two boundaries.

For the global model, we made 11-year integration for each month and annual mean forced by steady hydrography and wind stress respectively. For the North Pacific model we

Table 1. Depths and Thickness of Model Levels

Level	Depth range(m)	Thickness (m)	Mid~depth (m)
1	0~20	20	10
2	20~40	20	30
3	40~80	40	60
4	80~120	40	100
5	120~180	60	150
6	180~250	70	215
7	250~350	100	300
8	350~450	100	400
9	450~550	100	500
10	550~700	150	325
11	700~900	200	800
12	900~1100	200	1000
13	1100~1400	300	1250
14	1400~1750	350	1575
15	1750~2250	500	2000
16	2250~2750	500	2500
17	2750~3250	500	3000
18	3250~3750	500	3500
19	3750~4250	500	4000
20	4250~4750	500	4500
21	4750~5750	1000	5250

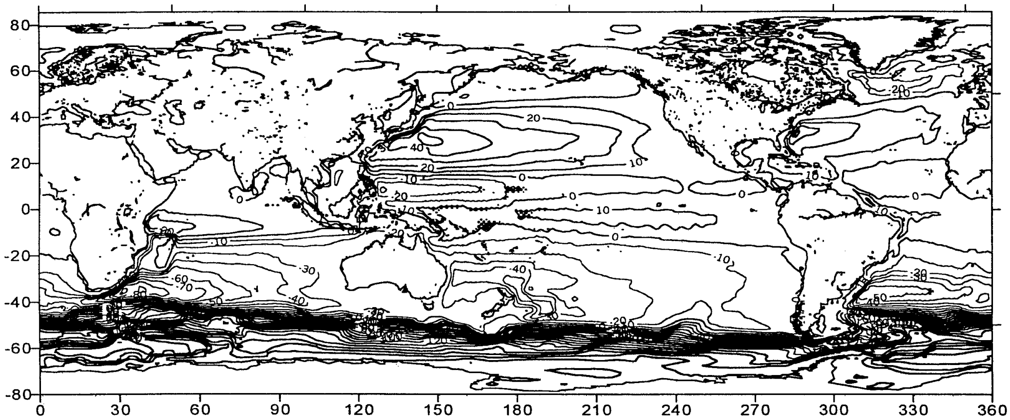

Fig. 1. Tranport stream function (unit: Sv) of the world ocean (annual mean)

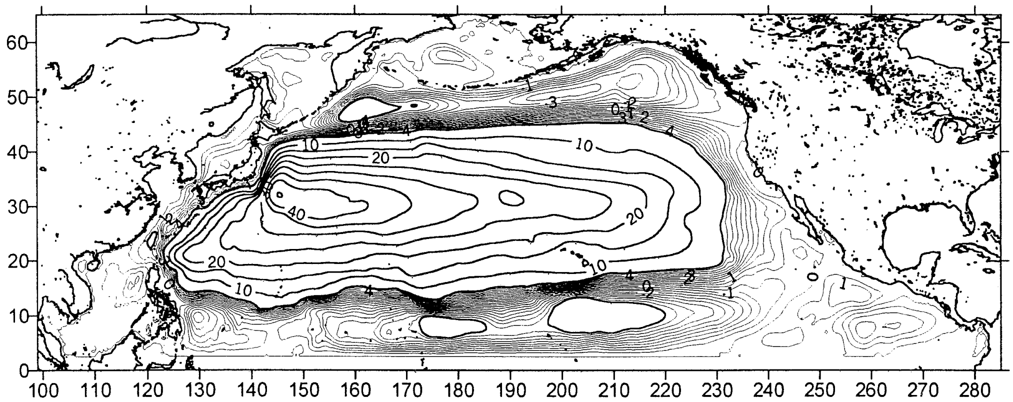

Fig. 2. Tranport stream function (unit: Sv) of the North Pacific (annual mean)

made 7-year integration. The results of the last year were saved for analysis.

3. Volume, heat and salt transports

The model-produced transport stream functions are shown in Figs. 1 and 2 respectively. From Fig. 1, we find that the basic pattern is quite similar to that of FUJIO *et al.* (1992), except that some improvement can be seen. For example, the western boundary currents are strengthened and thus more realistic, the Pacific equiatorial counter current and the Mindanao dome have been better reproduced. From Fig.2 we can see more detailed structures of the circulation near the western boundaries. These include the Mindanao dome southeast of Philippines, the NW Luzon Cyclonic Gyre in the South China Sea (FANG *et al.*, 1998), the Taiwan-Tsushima-Tsugaru Warm Current System in the East China Sea and Japan/East Sea (FANG *et al.*, 1991). These features were not resolved in FUJIO *et al.* (1992) due to its coarse grid.

To estimate the water volume, heat and salt transports in various regions we selected some representative sections in the oceans as shown in Fig. 3. The sections 1(C), 2(C) and 3(C) in the Pacific lie on the equator, 30° N and 30° S latitudes respectively. The transports across section 1(C) represent the energy and substance transfer between the North and South Pacific. These across section 2(C) represent energy and substance transfer between the northern and southern North Pacific. In particular, the heat transports here characterize the poleward heat flux in the Pacific. The

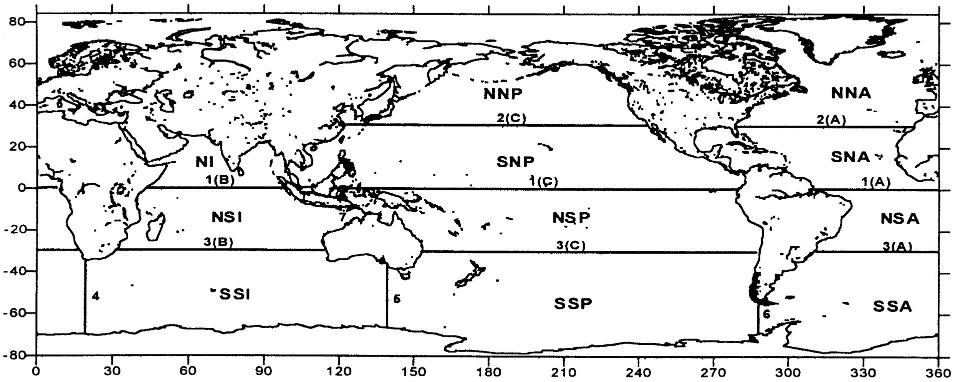

Fig. 3. The sections dividing the oceans into several regions

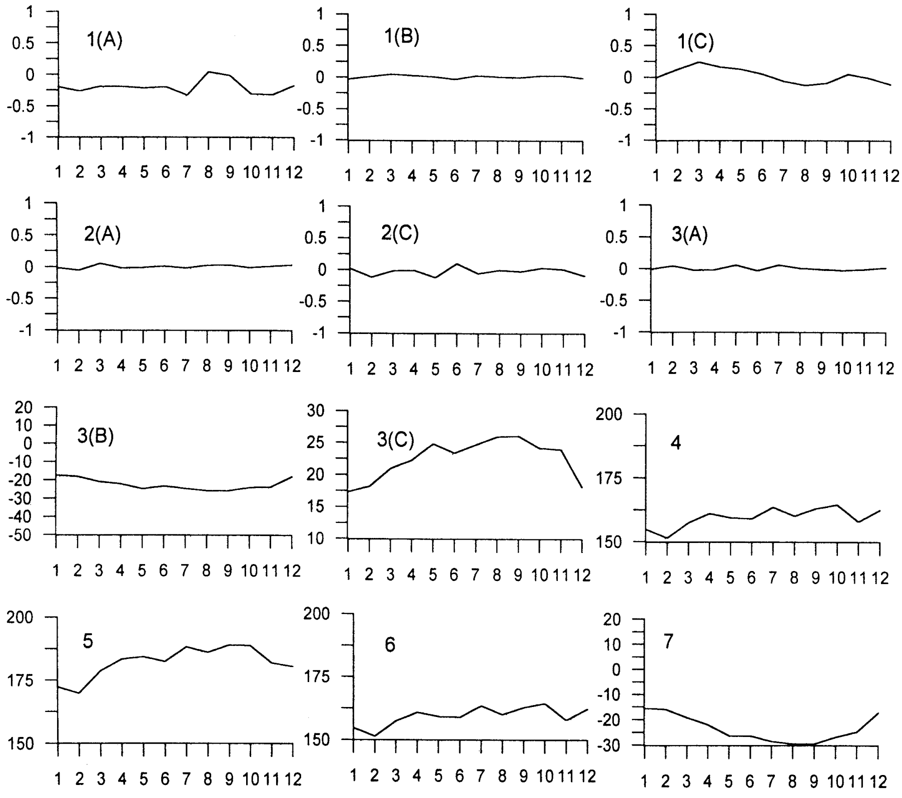

Fig. 4. The water volume transports (in Sv, 1 Sv $=10^6$ m^3/s) The abscissa denotes months

transports across section 3(C) represent the energy and substance transfer between the Pacific and the Southern Ocean. The sections in the Atlantic and Indian Oceans are similar. The sections 4, 5 and 6 separate the southern Atlantic, Indian and Pacific Oceans, while section 7 passes through the Indonesian Archipelago. For short, the regions separated by these sections are named as in Fig. 3.

Figures 4, 5 and 6 show the calculated water volume, heat and salt transports across the above representative sections. The unit is Sv(1 Sv $=10^6$ m^3/s) for the water volume transport, the unit for heat transport and salt transport

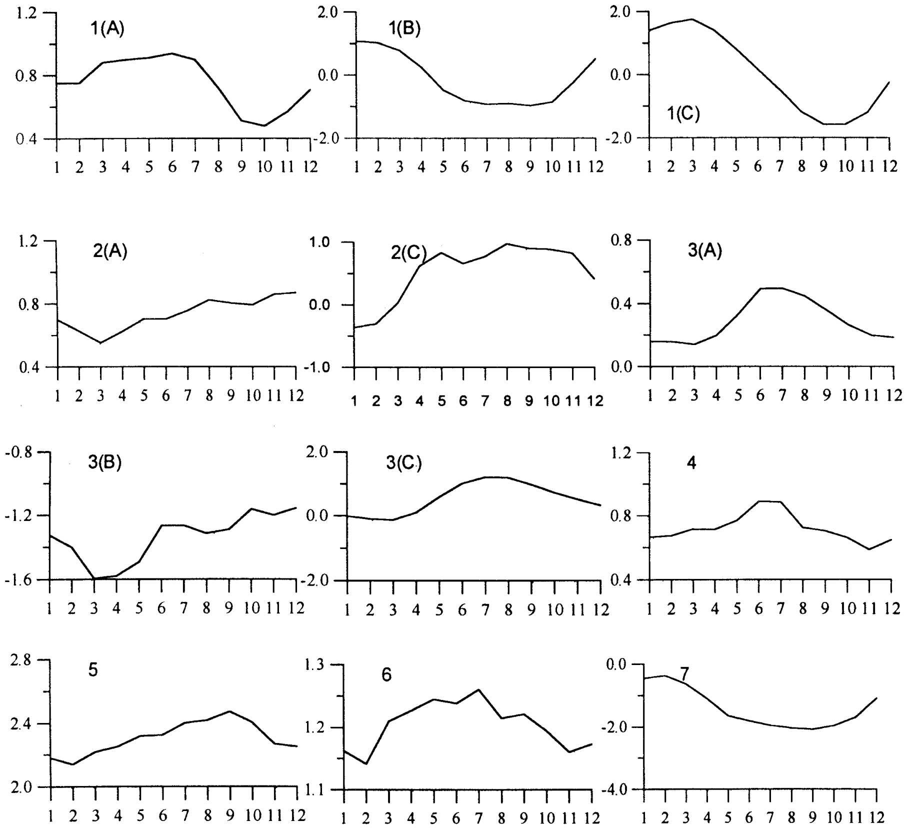

Fig. 5. The heat transports (in PW, 1 PW = 10^{15} W) The abscissa denotes months

are PW (1 PW = 10^{15} W) and Tg/s (Tera Grams /sec.) respectively. All these transports are denoted as positive if they are eastward and northward respectively.

The model result shows that: the Antarctic Circumpolar Current (ACC) has a volume transport of 170–220 Sv from the southern South Indian ocean (SSI) to the southern South Pacific (SSP), 150–180 Sv both from SSP to the southern South Atlantic (SSA) and from SSA to SSI. It indicates that there should be a pathway allowing the water to flow from the Pacific Ocean towards the Indian Ocean and then joining ACC and to return to the Pacific Ocean. By examining the transports across section 3(C), 7 and 3(B), we find that the transport from SSP to the northern South Pacific (NSP) is 17–26 Sv, the volume transport of the Indonesian Throughflow from the Pacific to Indian Ocean varies from 15 to 29 Sv, and that from the northern South Indian Ocean (NSI) to SSI is 17–26 Sv. This shows that the water volume transport is in balance. A rate of 15–29 Sv (with an average of 20 Sv) for the Indonesian Throughflow is rather close to the simulated result of GODFREY (1989) (16±4 Sv.) and the observational result of FIEUX *et al.* (1994) (18.6 ±7 Sv.).

Very small water flows across the equator in the Pacific, Atlantic and Indian Ocean, for that the northern boundaries of these oceans in the model are not connected to each other. For adjacent areas to the China, water is transported from the Pacific to the South China Sea through the Luzon Strait at rates of 0.6–2.1 Sv, and northward flows through the Taiwan Strait and east of the Taiwan Island are at 0.1 –1.9 Sv and 14–23 Sv respectively. Water flows from the East China Sea to the Pacific through the north of Ryukyu Island and to the East/

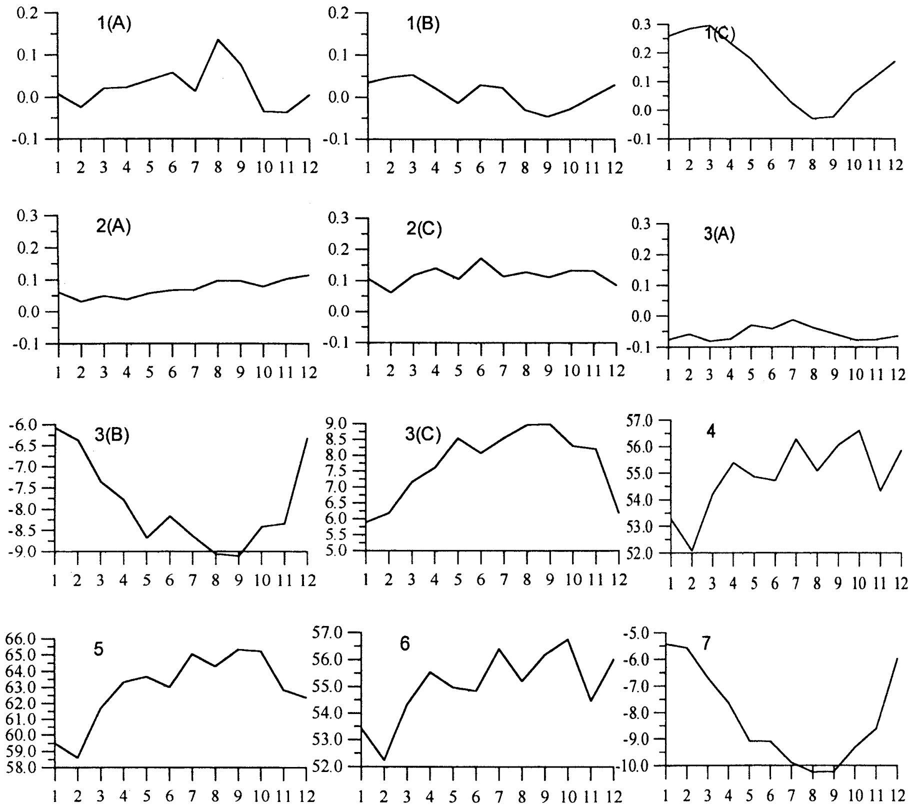

Fig. 6. The salt transports (in 10^{-1} Tera Grams/sec. (Tg/s)) The abscissa denotes months

Japan Sea through the Korea Strait are at 13–22 Sv and 1.6–2.1 Sv respectively. The volume transports from East/Japan Sea to the Pacific through the Tsugaru Strait and the Soya Stait are about 0.9 Sv and 0.5–1.0 Sv respectively.

The heat transport across the equator in the Atlantic Ocean is from 0.4 to 1.0 PW, and that in the Indian Ocean is from −1.0 to 1.0 PW. The heat transport across the equator in the Pacific Ocean varies from −1.5 PW in summer to 1.7 PW in winter. This seasonal characteristic is in agreement with the result of PHILANDER *et al.* (1987), who computed the seasonal variation of the zonally integrated meridional heat transport for the tropical Pacific Ocean. But our annual average of the cross-equator heat transport in the Pacific is lower than that calculated by PHILANDER *et al.* (1987). This is most likely a consequence of the negligence of the Indonesian Throughflow in the Philander's model. Across the latitude 30° N, the heat transport in the Pacific Ocean varies from −4.0 to 1.0 PW with an average of 0.5 PW. The heat transport in the Atlantic at 30° N varies from 0.5 to 0.9 PW with an average of 0.7 PW. YU and MALANOTTE-RIZZOLI (1998) calculated the heat transports in the North Atlantic using an inverse model. The annual average at 25° N is 0.7 PW, quite close to our result. In spite of large volume transport of ACC, the eastward heat transports of section 4, 5 and 6 are not accordingly large. The reason is that the temperature near the Antarctica is very low. The heat transport across section 5 is about 1 PW more than that across section 6. It indicates that a certian amount of heat in the SSP is lost. Checking the heat transport across the section 3(C), we find that about 1 PW is transferred from the Southern Ocean to the Pacific Ocean. Across the sections of 30° S, the heat transports in the Atlantic Ocean and Indian Ocean vary from 0.1 (in winter) to 0.5 (in summer) PW with an average of 0.3 PW and −1.0 to −1.6 PW with an average of −1.4 PW respectively. It means that across the latitude 30° S, the heat is transported northward in the Atlantic and Pacific Ocean, while southward in the Indian Ocean. These differences can be mainly attributed to the Agulhas Current and Indonesian Throughflow. The heat transport through the Indonesian Archipelago ranges from −2.0 PW to −0.4 PW, with annual average of −1.0 PW.

The salt transport across the equator vary from −0.002 Tg/s (in summer) to 0.03 Tg/s (in winter) in the Pacific Ocean, from −0.003 (in winter) to 0.014 Tg/s (in summer) in the Atlantic Ocean, and from −0.005 (in summer) to 0.005 Tg/s (in winter) in the Indian Ocean. Across the latitude 30° N, the salt transport in the Pacific Ocean is about 0.01 Tg/s with a small seasonal variation, and that in the Atlantic Ocean is from 0.003 to 0.01 Tg/s with a small seasonal variation too. Across the latitude 30° S, the salt transports are from −0.001 to −0.008 Tg/s in Atrantic Ocean, from −0.6 (in winter) to −0.9 Tg/s (in summer) in the Indian Ocean, and from 0.6 (in winter) to 0.9 Tg/s (in summer) in the Pacific Ocean. For ACC, the eastward salt transports across sections 4, 5 and 6 are very large. They are from 5.2 (in winter) to 5.65 Tg/s (in summer) iacross section 4, from 5.86 (in winter) to 6.53 Tg/s (in summer) across section 5, and from 5.22 (in winter) to 5.68 Tg/s (in summer) across section 6, This seasonal variation may be partially attributed to the variation in volume transports and may also be related with melt of the ice near the Antarctica in boreal winter, when the salinity of the seawater may decrease.

4. Concluding remarks

The 1-degree diagnostic model of the present study can well reproduce the basic patterns of the general circulation in the world ocean, the 1/3-degree model can significantly improve the results, especially in producing the structures of the circulation in the Pacific-Asian marginal seas.

Though the cross-equator transports in the Atlantic, Indian and Pacific Ocean are all small, the heat transports across equator in the Atlantic is northward. This is clearly a result of the southward flow of the North Atlantic Deep Water and the northward compensative warm flow in the upper layer. The annual mean of the cross-equator heat transport in the Pacific from the present model is significantly lower than that calculated by PHILANDER *et al.* (1987). This might indicate the importance of the indonesian Throughflow in the heat transport in the Pacific. Our calulation shows that the heat transport through the Indonesian Archipelago is −1.0 PW, which is comparable with the poleward heat transport in the North Atlantic and Pacific Oceans. The difference in heat transports across the sections 4 and 5 demonstrates the important role of the Agulhas Current in the heat balance of the world ocean.

Nevertheless the present work did not well reproduce some observational features, for example, the position of the Kuroshio deviates eastward. This is likely a result of the coarse resolution in the available climatological hydrographic data. To better simulate the western boundary current diagnostically a refined temperature and salinity climatological dataset is resuired.

Acknowledgments

The present work was supported by the National Science Foundation of China Grants 49876010 and 49576280, the Major State Basic Research Program, No.G1999043808 and the Chinese Academy of Sciences Grant KZCX 2-202-01. The work was also partially supported by Natural Hazard Prevention Research (Critical Technology-21) Project, funded by MOST through KISTEP (Korea Institute of Science and Technology Evaluation Planning) and Daewoo Corporation, Korea for the second author.

References

BRYAN, K. (1969): A numerical method for the study of the circulation of the world ocean, Journal of Computational Physics, **4**, 347-376.

FANG, G. *et al.* (1998): A survey of studies on the South China Sea upper ocean circulation. Acta Oceanographica Taiwanica, **37**(1), 1-16.

FANG, G. *et al.* (1991): Water transport through the Taiwan Strait and the East China Sea measured with current meters. Oceanography of Asian marnginal Seas (TAKAN, T. ed.) Elsevier, Holland, 345–358.

FIEUX, M. *et al.* (1994): Measurements within the Pacific–Indian oceans throughflow region. Deep Sea Res., Part I, **41**, 1091–1130.

FUJIO, S. and N. IMSASATO (1991): Diagnostic calculation for circulation and water mass movement in the deep Pacific. J. Geophys. Res, **96**, 759–774.

FUJIO, S. *et al.* (1992): World ocean circulation diagnostically derived from hydrographic and wind stress fields, 1. The velocity field. J. Geophys. Res, **97**, 11163–11176.

FUJIO, S. *et al.* (1992): World ocean circulation diagnostically derived from hydrographic and wind stress fields, 2. The water movement. J. Geophys. Res, **97**, 14439–14452.

GODFREY, J. S.(1989): A Sverdrup model of the depth integrated flow for the world ocean allowing for island circulations. Geophys. Astrophys. Fluid Dyn., **45**, 89–112.

HELLERMAN, S., and M. ROSENSTEIN (1983): Normal monthly wind stress over the world ocean with error estimates. Jpurnal of Physical Oceanography, **13**, 1093–1104.

PHILANDER, S., W. J. HURLIN and A. D. SEIGEL (1987): Simulation of the seasonal cycle of the tropical Pacific ocean. Journal of Physical Oceanography, **17**, 1986–2002.

SARMIENTO, J. L. and K. BRYAN (1982): An ocean transport model for the North Atrlantic. J. Geophys. Res, **87**, 394–408

SEMTNER, A. J. and R. M. CHERVIN (1988): A simulation of the global ocean circulation with resolved eddies. J. Geophys. Res., **93**, 15502–15522.

SEMTNER, A. J., Jr., and R. M. CHERVIN (1992): Ocean general circulation from a global eddy–resolving model. J. Geophys. Res. **97**, 54493–5550

YU, L. and P. MALANOTTE–RIZZOLI (1998): Inverse modeling of seasonal variations in the North Atlantic Ocean. J. Phys. Oceanogr, **28**, 902–922.

Received on May 23, 2000
Accepted on October 31, 2000